J. Mountain Res. P-ISSN: 0974-3030, E-ISSN: 2582-5011 DOI: https://doi.org/10.51220/jmr.v16i2.34
Vol. 16(2) Special Issue ICRAMS-2021, (2021), 279-286

Investigation on Dielectric and Optical Properties of $Ba_{1-x}Ca_xZr_{0.1}Ti_{0.9}O_3$ (x = 0.150) Ferroelectric Ceramics

Don Biswas[1,2*] • Surendra Singh[1] • Prashant Thapliyal[1] • Vishal Rohilla[1] • G S Kathait[1] • N S Panwar[1] • Prolay Sharma[2]

[1]*Instrumentation Engg.-USIC, H.N.B. Garhwal University, Srinagar – 246174, India.*
[2]*Instrumentation and Electronics Engg., Jadavpur University, Kolkata, India.*

***Corresponding author Email:** donusic06@gmail.com

Received: 29.8.2011; Revised: 22.11.2021; Accepted: 27.11.2021

Abstract: Pellet samples of $(Ba_{1-x}Ca_xZr_{1-y}Ti_y)O_3$ (x = 0.150, y = 0.90) were prepared using the solid-state reaction method following double sintering. The electrical and optical properties of $(Ba_{1-x}Ca_xZr_{1-y}Ti_y)O_3$ (x = 0.150, y = 0.90) ceramics were studied. For $(Ba_{0.85}Ca_{0.15}Zr_{0.1}Ti_{0.9})O_3$ ferroelectric perovskite ceramics, the dielectric and structural properties were explored. The prepared composition of BCZT ceramics were calcined at 1100 ºC. The sintering temperature was 1300 ºC. Dielectric properties were observed from room temperature (RT) to 150 ºC, at 1 MHz. The powder of the sintered samples has been taken for reflectance measurement at UV-Vis range. From the observed tauc plot, the band-gap is calculated. The measured band- gap is 3.19 eV.

Keywords- Dielectric constant; Electric conductivity; Reflectance; UV-Vis.

Introduction

Perovskite compounds are of considerable interest due to their high extent of tailorability in physical properties and application in the field of sensors. Their contributions in the field of sensors are significant due to their large piezoelectric properties. Ferroelectric/ABO_3 type materials may generate voltage if external voltage or pressure has been applied to it. These compounds possess spontaneous polarization.

Researchers investigated the dielectrics properties of $(Ba_{1-x}Ca_xZr_{1-y}Ti_y)O_3$ (x = 0.150, y = 0.90) ceramics, near morphotropic phase boundary (MPB) region (Tian et al., 2013; Mondal et al., 2017; Hennings and Schnell, 1982; Yu et al., 2002; Wang et al., 2012; Wu et al., 2012). The BCZT ceramics show significant dielectric properties, at x = 0.150. At x = 0.150, Tian et al. observed co-existence of two different phases in BCZT ceramics (Tian et al., 2013). For $(Ba_{0.85}Ca_{0.15}Zr_{0.1}Ti_{0.9})O_3$ samples, O ("Orthorhombic")- T ("Tetragonal") transition point has been observed near 120 ºC (Tian et al., 2013). The presence of these phases may create several possible polarization directions. Therefore, this MPB consisting of both phases and may have maximum possible polarization directions, which may contribute towards k_s (coupling

factor). A significant dielectric constant may be seen because of its large remnant polarization, which increases due to its large coupling factor (Yamashita and Shimanuki, 1996; Yamashita et al., 1996; Yamashita et al., 1998).

In this study, the $(Ba_{1-x}Ca_xZr_{1-y}Ti_y)O_3$ (x = 0.150, y = 0.90) samples were prepared using the conventional "solid- state reaction" method with double sintering. The pellet samples were sintered at 1300 °C for 4 hrs. For dielectric measurement, the pellet samples were electroded with conducting silver paste, in M-I-M configuration. For XRD measurement, the prepared powder sample of BCZT composition was taken. Furthermore, PANalytical, X'PERT PRO X-ray machine has been used to measure XRD patterns. It has Cu$K_{\alpha 1}$ radiation of wavelength 1.54060 Å. The range of 2θ angle was selected from 20 to 70°, at a scanning rate 0.3 sec per step with step size 0.03°.

Experimental details

The pellet samples of $(Ba_{1-x}Ca_xZr_{1-y}Ti_y)O_3$ (x = 0.150, y = 0.90) were prepared using solid-state reaction method with double sintering. Raw materials of Barium carbonate ($BaCO_3$), Calcium carbonate ($CaCO_3$), Zirconium oxide (ZrO_2), and Titanium oxide (TiO_2) were taken with purity 99.99%, were dried at 200 °C for 2 hours to remove the absorbed moisture. The methodology has been described in a previous communication (Biswas et al., 2020; Biswas et al., 2021; Biswas et al., 2019; Biswas et al., 2018; Biswas et al., 2021; Singh et al., 2018; Singh et al., 2019).

Result and discussion

X- Ray Diffraction result

The XRD measurement was carried out for the $(Ba_{1-x}Ca_xZr_{1-y}Ti_y)O_3$ (x = 0.150, y = 0.90) composition, at the selected 2θ angle range. It has been shown in Fig. 1. For the prepared composition, powder sample was found in good consistency with "Inorganic Crystal Structure Database" (ICSD file No. 00-056-1033) data (Sen and Choudhary, 2004), with peaks corresponding to (020), (221), (402). The measured RT- XRD data of the $(Ba_{0.85}Ca_{0.15}Zr_{0.1}Ti_{0.9})O_3$ powder samples exhibit orthorhombic phase.

The lattice parameters were measured manually. The selected space group is 'C' type. For the prepared powder samples, the measured X- ray diffraction data were matched with "Inorganic Crystal Structure Database" (ICSD) data. The ICSD data will give the information of the orthorhombic unit cell (a, b and c parameters) and volume. The manually calculated values (a, b and c parameters) must be in more close approximation to those values. At first, the positions of the observed x- ray peaks were

identified. For a corresponding peak, the d-spacing and (hkl) has been noted from the ICSD data. The equation for an interplaner spacing for an orthorhombic unit cell was used to calculate the lattice parameters. To work with the above interplaner equation, the h, k, l, and d values were noted and further, the lattice parameters were measured. The lattice parameters were given in Table 1.

Table 1. Lattice parameters of $(Ba_{1-x}Ca_xZr_{1-y}Ti_y)O_3$ (x = 0.150, y = 0.90) samples and peaks used in the present calculation were (111), (020) and (402).

Cell Constants (Calculated)

$(Ba_{0.85}Ca_{0.15}Zr_{0.1}Ti_{0.9})O_3$	a (Å)	b (Å)	c (Å)	c/a (Å)
0.150	9.89054	5.61610	6.71288	0.67871

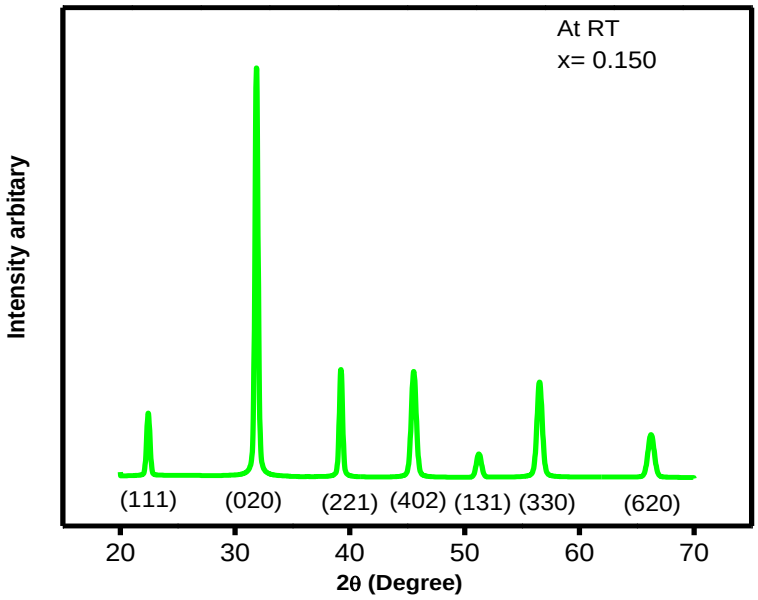

Fig. 1. XRD patterns of $(Ba_{1-x}Ca_xZr_{1-y}Ti_y)O_3$ (x = 0.150, y = 0.90) ceramics, at room temperature.

Dielectric and morphology results

In this study, the relative permittivity (K), loss tangent (tan δ), and dielectric conductivity (σ) were observed systematically. For the prepared samples, K, tan δ, and σ were measured from temperature 30 and 140 ºC, at 1 MHz (Figs. 2- 3). The micro- structure show fine grain and homogeneous structure of the $(Ba_{0.85}Ca_{0.15}Zr_{0.1}Ti_{0.9})O_3$ samples. The grain size was observed between 0.7 and 1.0 µm (Fig. 4). The average grain size was measured 1.15 µm. The dielectric constant was found maximum near 120 ºC.

Furthermore, the dielectric constant has been decreasing with an increase in temperature. The large value of the dielectric constant indicates a phase change near 120 °C. The transition is also observed from the data of electric conductivity. The electric conductivity was suddenly increased near 120 °C and further, it decreases. The loss of the prepared composition is very small at high frequency.

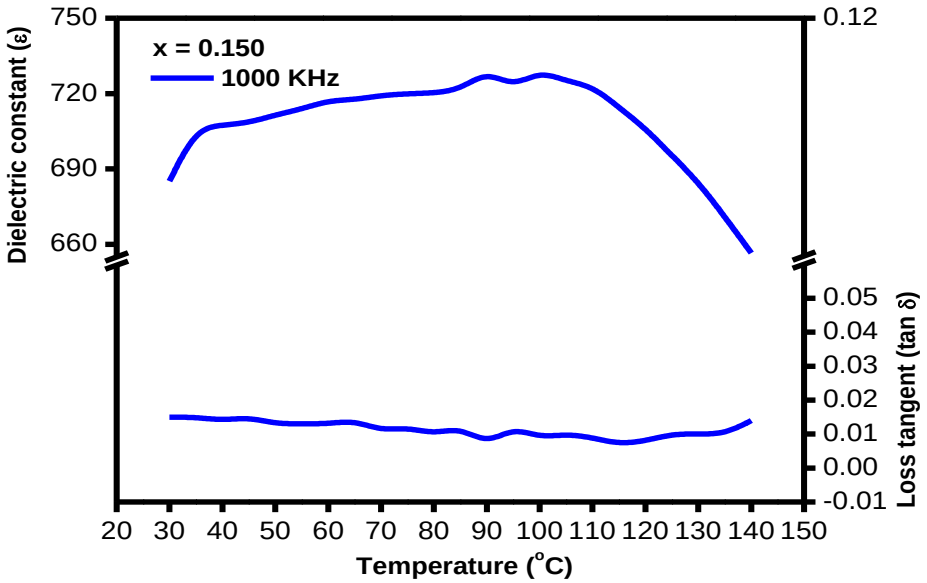

Fig. 2. Temperature- dependent dielectric constant and loss tangent of the $(Ba_{1-x}Ca_xZr_{1-y}Ti_y)O_3$ (x = 0.150, y = 0.90) sample, at 1 MHz.

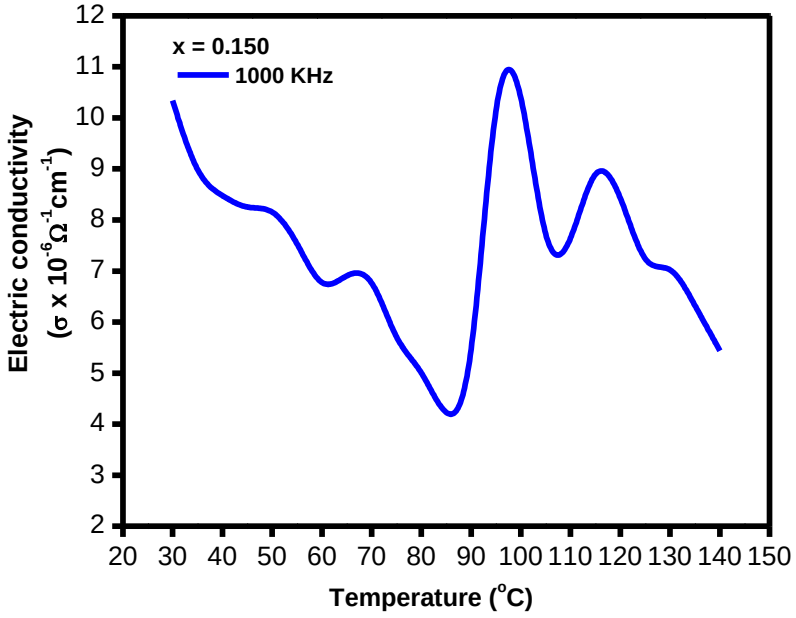

Fig. 3. Temperature- dependent electric conductivity of the $(Ba_{1-x}Ca_xZr_{1-y}Ti_y)O_3$ (x = 0.150, y = 0.90) ceramics, at 1 MHz.

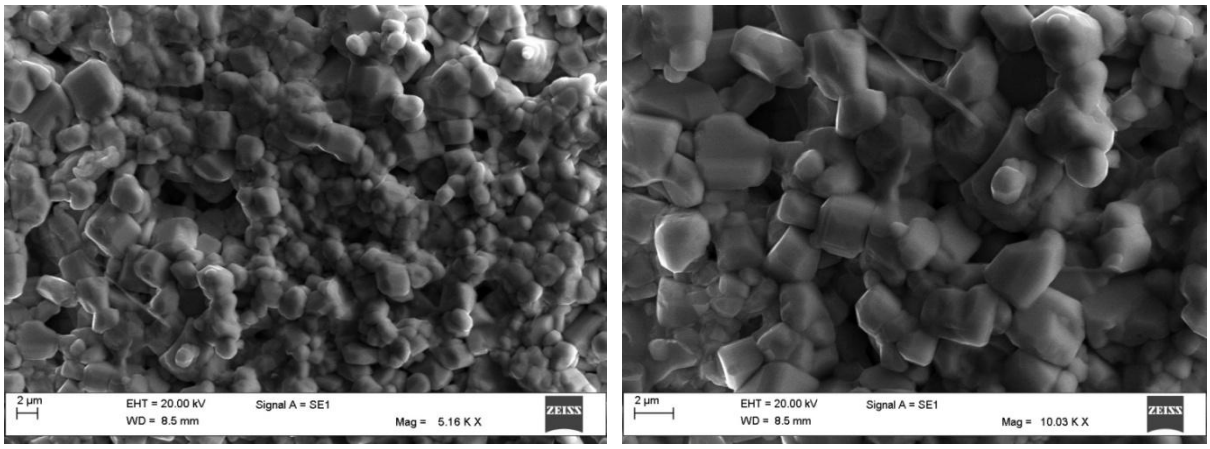

Fig. 4. SEM images of $(Ba_{1-x}Ca_xZr_{1-y}Ti_y)O_3$ (x = 0.150, y = 0.90) ceramics, at different magnification.

Table 2: Energy dispersive X- ray results of the $(Ba_{1-x}Ca_xZr_{1-y}Ti_y)O_3$ (x = 0.150, y = 0.90) system and spectrum analysis.

ELEMENT	WEIGHT%	ATOMIC%
O K	25.69	66.10
Ca K	2.39	2.46
Ti K	16.36	14.06
Zr L	4.81	2.17
Ba L	50.75	15.21
Totals	100.00	

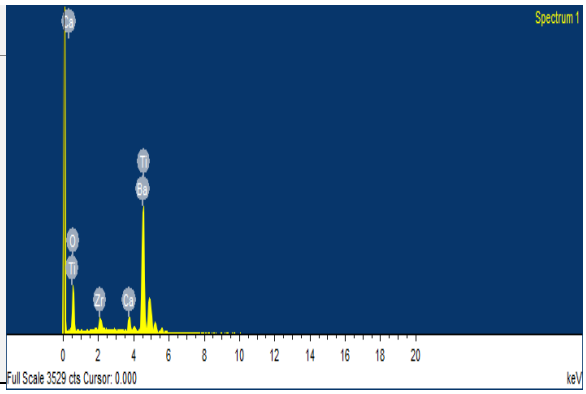

Table 3. Standards selected in EDAX analysis of the $(Ba_{1-x}Ca_xZr_{1-y}Ti_y)O_3$ (x = 0.150, y = 0.90) ceramics.

STANDARD DETAILS			
O	SiO2	01.06.1999	12 AM
Ca	Wollastonite	01.06.1999	12 AM
Ti	Ti	01.06.1999	12 AM
Zr	Zr	01.06.1999	12AM
Ba	BaF2	01.06.1999	12 AM

Lossy dielectric can be characterized with the help of a circuit analog of a resistance in parallel with a capacitor (Haertling, 1967). When the input signal is taken as a sinusoidal signal, the capacitor always show low reactance path at higher frequencies, leading to minimization in conduction losses. Therefore, dielectric loss has been decreasing with an increase in frequency, which is consistent with the previous reports (Haertling, 1967; Jaeger and Egerton, 1962). The EDAX results confirmed the atomic percentage of the elements. The data has been given in Table 2. From the spectrum of EDAX, the presence of the elements can be confirmed. The standard details were given below in Table 3.

Reflectance results

The optical properties of the prepared composition have been observed (Figs. 5-6). The band-gap was measured 3.19 eV (Tunc et al., 2019). The band-gap is calculated using tauc function. Fig. 4 indicates the reflectance graph with the variation in wavelength. The reflectance is 75% at around 900 nm (UV range) and 10% at around 350 nm (Vis range). A sharp downfall may be observed in reflectance plot at around 350 nm. Teflon is taken as the standard material.

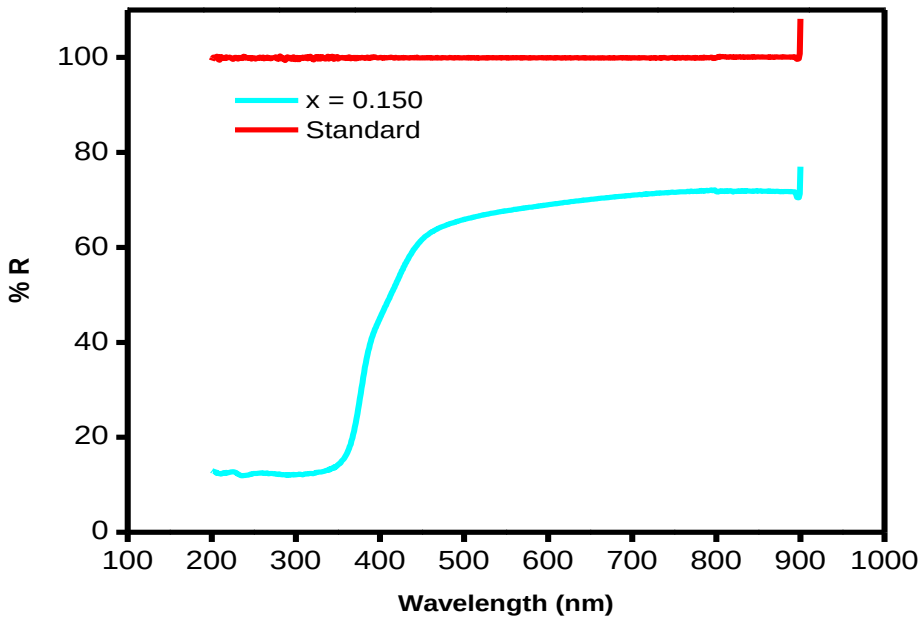

Fig. 5. Variation in reflectance with the wavelength, in $(Ba_{1-x}Ca_xZr_{1-y}Ti_y)O_3$ (x = 0.150, y = 0.90) ceramics, at 1 MHz.

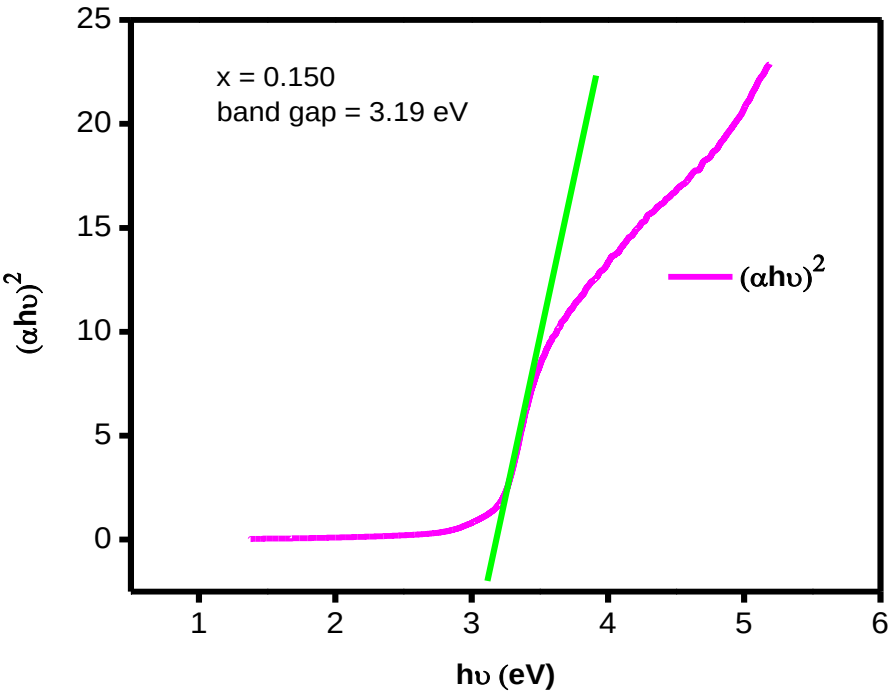

Fig. 6. Tauc plot of the $(Ba_{1-x}Ca_xZr_{1-y}Ti_y)O_3$ (x = 0.150, y = 0.90) powder samples.

Conclusion

The dielectric and optical properties of the ferroelectric perovskite $(Ba_{0.85}Ca_{0.15}Zr_{0.1}Ti_{0.9})O_3$ ceramics were observed. The composition shows polycrystalline structure. The observed maximum dielectric constant is measured 729, at around 100 ^oC. Also grain size is in µm range. From the observed optical properties, the reflectance was observed 80% near UV wavelength and 10% near visible range. The band-gap of the prepared composition is 3.19 eV.

References

Biswas D, Panwar NS and Sharma P (2020). Converse piezoelectric properties of lead free $Ba_{1-x}Ca_xZr_{0.1}Ti_{0.9}O_3$ (x = 0.055) ceramics using double sintered method. *Ferroelectrics* 568: 95-103.

Biswas D, Sharma P and Panwar NS (2021). Dielectric properties of $Na_{1-x}K_xNbO_3$ (NKN) (0.160 ≤ x ≤ 0.200) ceramics synthesized by double sintered method. *Ferroelectrics* 571: 214- 229.

Biswas D, Kathait GS, Thapliyal P, Rohilla V, Singh S and Negi J (2019). Converse piezoelectric properties of K and Na-modified $(Na_{1-x}K_x)$ NbO_3 lead free ceramics for x = 0.08 and 0.17. *Ferroelectrics* 550: 228–232.

Biswas D, Kathait GS, Thapliyal P, Rohilla V and Singh S (2018). Temperature dependence of dielectric properties of sodium potassium niobate ceramics for different values of x $(Na_{1-x}K_xNbO_3)$. *Ferroelectrics* 526: 168-175.

Biswas D, Sharma P and Panwar NS (2021). Structural and electrical properties of lead free $Na_{1-x}K_xNbO_3$ (0.160 ≤ x

≤ 0.200) ceramics. *Ceramics International* 47: 13814–13819.

Haertling GH (1967). Properties of hot-pressed ferroelectric alkali niobate ceramics. *J. Am. Ceram. Soc.* 50: 329.

Hennings D and Schnell A (1982). Diffuse Ferroelectric Phase Transitions in $Ba(Ti_{1-y}, Zr_y)O_3$ Ceramics. *J. Am. Ceram. Soc.* 65: 539–44.

Jaeger RE and Egerton L (1962). Hot pressing of potassium-sodium niobates. *J. Am. Ceram. Soc.* 45: 209.

Mondal T, Das S, Badapanda T, Sinha TP and Sarun PM (2017). Effect of Ca^{2+} substitution on impedance and electrical conduction mechanism of $Ba_{1-x}Ca_xZr_{0.1}Ti_{0.9}O_3$ ($0.00 \leq x \leq 0.20$) ceramics. *Physica B.* 508: 124-135.

Negi J and Panwar NS (2021). Structural and electrical properties of lead-free $Na_{0.685}K_{0.315}Nb_{1-y}Ta_yO_3$ ($0 \leq y \leq 0.05$) ceramics. *Journal of Physics and Chemistry of Solids* 151: 109853.

Singh S, Negi J and Panwar NS (2018). Dielectric properties of $Na_{1-x}K_xNbO_3$, near x = 0.5 morphotropic phase region. *Journal of Physics and Chemistry of Solids* 123: 311-317.

Singh S, Negi J and Panwar NS (2019). Temperature dependent dielectric properties of (Na, K) NbO_3, near equimolar composition, *Ceramics International* 45: 13067–13071.

Sen S and Choudhary R (2004). Effect of doping Ca ions on structural and electrical properties of $Ba(Zr_{0.05}Ti_{0.95})O_3$ electroceramics. *J. Mater. Sci.: Mater Electron* 15: 671-675.

Tian Y, Wei L, Chao X, Liu Z and Yang Z (2013). Phase Transition Behavior and Large Piezoelectricity Near the Morphotropic Phase Boundary of Lead-Free $(Ba_{0.85}Ca_{0.15})(Zr_{0.1}Ti_{0.9})O_3$ Ceramics. *J. Am. Ceram. Soc.* 96: 496–502.

Tunc S, Sonmez NA, Cetin SS and Ozcelik S (2019). Influences of annealing temperature on anti-reflective performance of amorphous Ta_2O_5 thin films. *Ceramics International* 45: 11-18.

Wang P, Li Y and Lu Y (2011). Enhanced piezoelectric properties of $(Ba_{0.85}Ca_{0.15})(Ti_{0.9}Zr_{0.1})O_3$ lead-free ceramics by optimizing calcination and sintering temperature. *J. Eur. Ceram. Soc.* 31: 2005–2012.

Wu J, Xiao D, Wu B, Wu W, Zhu J, Yang Z and Wang J (2012). Sintering temperature-induced electrical properties of $(Ba_{0.90}Ca_{0.10})(Ti_{0.85}Zr_{0.15})O_3$ lead-free ceramics. *Mater. Res. Bull.* 47: 1281–1284.

Yamashita Y and Shimanuki S (1996), Synthesis of lead scandium niobate-lead titanate pseudo binary system single crystals. *Mater. Res. Bull.* 31: 887–895.

Yamashita Y, Harada K, Tao T and Ichinose N (1996). Piezoelectric properties of the $Pb(Sc_{1/2}Nb_{1/2})$ O_3-$Pb(Mg_{1/3}Nb_{2/3})$ O_3-$PbTiO_3$ ternary ceramic materials near the morphotropic phase boundary. *Integrated Ferroelectrics* 13: 9–16.

Yamashita Y, Harada K, Hosono Y, Natsume S and Ichinose N (1998). Effects of B-site Ions on the Electromechanical Coupling Factors of $Pb(B'B'')O_3$–$PbTiO_3$ Piezoelectric Materials. *Jpn. J. Appl. Phys.* 37: 5288–5291.

Yu Z, Ang C, Guo R and Bhalla AS (2002). Piezoelectric and Strain Properties of $Ba(Ti_{1-x}Zr_x)O_3$ Ceramics. *J. Appl. Phys.* 92: 1489–93.